Modeling and simulation of chemical reactions at the surface of an ablative wall interacting with a hypersonic flow.

CORIA Guillaume[*] _and Dr PARISSE Jean-Denis_[†]
French Air Force Academy, Base Aérienne 701, Salon Air, 13661, France

Dr LAMET Jean-Michel[‡] _and Dr DELLINGER Nicolas_[§]
ONERA/Département Multi-Physique pour l'Énergétique, Université de Toulouse, F-31055, Toulouse, France

Abstract

THIS paper focuses on the modeling and simulation of chemical reactions of oxidation, nitridation and sublimation at the surface of an ablative Thermal Protection System (TPS) interacting with a hypersonic flow of Earth's atmosphere. After a description of the chosen chemical models, models are described and validated on a simple test case using an uncoupled in-house software. Then, to simulate the interaction between the TPS and the hypersonic flow, three softwares developed at French aerospace research lab (ONERA) are used. To model the thermal degradation of TPSs' composite materials, the MoDeTheC solver, in which models of thermokinetic degradation and surface chemical reactions are implemented, is used. To model the hypersonic flow, the CEDRE platform and in particular the Navier-Stokes CHARME solver are used. To ensure coupling between the ablative TPS and the hypersonic flow, the coupling library CWIPI is used to interface MoDeTheC and CHARME. Finally, results obtained by coupling MoDeTheC and CHARME are analyzed and compared to reference data available in the literature for the experimental flight Radio Attenuation Measurements project C probe I (RAMC-I).

---

[*]PhD student, Centre de Recherche de l'École de l'air, guillaume.coria@ecole-air.fr

[†]Associate Professor, Centre de Recherche de l'École de l'air, jean-denis.parisse@ecole-air.fr

[‡]Research engineer, Multi-Physics for Energetics Department, ONERA, jean-michel.lamet@onera.fr

[§]Research engineer, Multi-Physics for Energetics Department, ONERA, nicolas.dellinger@onera.fr

Nomenclature

Physics constants

h	Planck's constant	$6.62607015 \times 10^{-34}$ J.s^{-1}
k	Boltzmann's constant	1.380649×10^{-23} J.K^{-1}
N_a	Avogadro's constant	$6.02214076 \times 10^{23}$ mol^{-1}
N_S	Number of site per square meter	3.56×10^{19} m^{-2}
P_0	Standard pressure	101 325 Pa

Other symbols

$\dot{m}$	Mass flow rate	kg.s^{-1}.m^{-2}
μ	Stoichiometric coefficient (Positive in products, negative in reactants)	
ρ	Volumic mass	kg.m^{-3}
τ	Surface reaction rate	mol.m^{-2}.s^{-1}
θ	Fraction of free sites	
θ_x	Fraction of sites occupied by species x	
K	Equilibrium constant of chemical reactions	
k_f, k_b	Constants of direct and reverse reactions	
K_f	Formation constant	J.mol^{-1}
m	Mass	kg
N_s	Sites number per square meter	m^{-2}
P	Pressure	Pa
P_x	Partial pressure of species x	Pa
T	Temperature	K
T_d	Activation energy of reaction	K
V_{reg}	Regression speed	m.s^{-1}

1. Introduction

The atmospheric reentry of space objects is the place of many physical phenomena which immerse them to extreme conditions. The strong detached shock created ahead space objects transmits very large heat fluxes to the TPS. The huge energy to be dissipated (of the order of several mega-Joule) requires the use of TPS made of ablative materials (generally carbon-based composites) to ensure the survival of the objects' structure. The multi-physical character and the extreme conditions intrinsic to ablation make it difficult to investigate those phenomena in laboratory or in test flight. Even today, TPS design is based on important safety factors. Numerical simulation appears to be an essential tool for reducing these safety margins, and, among others, the weight in the TPS design. This paper is part of this process of improving computational tools related to ablation degradation.

The present work is devoted to the modeling and simulation of the degradation, due to pyrolysis and surface chemical reactions, of ablative carbon composite materials used as TPS for hypersonic reentry vehicles. Detailed models of oxidation, nitridation and sublimation of Duffa [1] and Zhluktov [2] are implemented in the finite volume material response solver used to model thermal degradation of composites (MoDeTheC) [3], developed at the ONERA. In order to simulate thermal degradation and surface regression of the TPS, the strategy is based onto a coupling between MoDeTheC and the multi-physics platform CEDRE [4] using the Computational Fluid Dynamic (CFD) Navier-Stokes solver CHARME, also developed at ONERA. The chosen chemical models introduce 12 reactions as well as the notion of reactive sites on the TPS surface. A site is a free surface carbon bond resulting from the composition of the material (carbon fibers for example) or from its degradation (by pyrolysis for example). These models are firstly validated on a simple test case at atmospheric pressure which consist in applying the composition and temperature of the Earth's atmosphere at the thermodynamic equilibrium to an elementary surface of a phenolic carbon TPS modeled in the MoDeTheC solver. Secondly, the material response, coupled with the hypersonic flow in the CEDRE platform, is compared to reference data available in the literature for the experimental flight RAMC-I carried out by National Aeronautics and Space Administration (NASA) [5, 6]. Simulation of the trajectory point at the altitude of 40 km and Mach 23.474 has been performed using the SATOR supercomputer of ONERA. The Earth's atmosphere is modeled by Park's model [7] of a mixture of viscous and reactive ideal gases (11 species and 23 chemicals reactions) which can be laminar or turbulent ($k - \omega$ model). The coupling strategy consists in the exchange of pressure, chemical composition, heat fluxes, pyrolysis gases fluxes, ablation mass and energy fluxes and temperature of the wall and of the gases at the coupling interface. The results of the simulation determine the regression rate of the wall as well as the characterization of the interaction between the flow and the TPS.

2. Chemical models

This paper focuses on the chemical reactions at the surface of a TPS. Three kinds of processes can occur according to external conditions and material temperature: oxidation, nitridation and sublimation. First of all, surface oxidation (respectively nitridation) is the reaction between an atom or molecule containing oxygen (respectively nitrogen) and the TPS, or more specifically, the carbon atoms of the wall surface. Sublimation, of solid carbon in our studies, corresponds to phenomenon of change of state from the solid directly to the gaseous state of the TPS. Pyrolysis is a chemical reaction occurring under the only action of the rise of temperature in the organic compounds. Thus, in the materials constituting thermal protection, the resin of composites is subject to this reaction which can be written in the form :

$$\text{Virgin material} \xrightarrow{\ ^\circ \text{K}\ } \text{Pyrolysis gaz + Char}$$
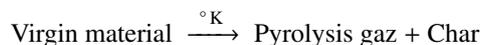
In addition, the hot gases released into the environment contribute to the removal of heat. Two models have been selected in the literature to be implemented in MoDeTheC solver, namely the models of Duffa [1] and V. Zhluktov [2]. They both describe kinetic reactions that occur at the TPS surface and provide the surface mass flow rate of carbon (kg.m^{-2}.s^{-1}) from which the regression rate of the wall (m.s^{-1}) is deduced. They also give access to the surface mass flow rates of involved gaseous species exchanged between the flow and the wall.

2.1 Duffa Model

Duffa [1] describes every reactions using the concept of active site. A site corresponds to an available bond of a carbon atom at the wall surface. These carbon bonds come directly from the composite material (carbon fiber) or from the degradation of its resin by pyrolysis for example. This model assumes that each site has the same chemical potential, i.e. each site has the same probability of reacting with a molecule or atom, and can be bound with an oxygen atom (Site $-$ O) or nitrogen atom (Site $-$ N). The reactions taken into account are gathered in Table 1. Note that reactions are assumed to be reversible. In Table 1 Cs represent a carbon atom at solid state and C at gas state. This model uses

ABLATIVE TPS INTERACTING WITH A HYPERSONIC FLOW

Arrhenius' laws to determine the kinetic constants of direct reactions k_{fi} and reverse reactions k_{bi} derived from the interaction mechanisms of Eley-Rideal and Langmuir-Hinshelwood detailed in the table 1.

Table 1: Surface reactions of Duffa's model [1]

	Reactions' expression	Reactions' rate
Reaction R_1	$2\,\text{Site} + \text{O}_2 \rightleftharpoons 2\,\text{Site}-\text{O}$	$N_a\tau_1 = k_{f_1}\theta^2 p_{\text{O}_2} - k_{b_1}\theta_O^2$
Reaction R_2	$\text{Site}-\text{O} \rightleftharpoons \text{Site} + \text{O}$	$N_a\tau_2 = k_{f_2}\theta_O - k_{b_2}\theta p_{\text{O}_2}$
Reaction R_3	$\text{Site}-\text{O} + \text{O} \rightleftharpoons \text{Site} + \text{O}_2$	$N_a\tau_3 = k_{f_3}\theta_O p_O - k_{b_3}\theta p_{\text{O}_2}$
Reaction R_4	$\text{Site}-\text{O} + \text{CO} \rightleftharpoons \text{Site} + \text{CO}_2$	$N_a\tau_4 = k_{f_4}\theta_O p_{\text{CO}} - k_{b_4}p_{\text{CO}_2}\theta$
Reaction R_5	$\text{Site}-\text{O}\,(+\,\text{Cs}) \rightleftharpoons \text{Site} + \text{CO}$	$N_a\tau_5 = k_{f_5}\theta_O - k_{b_5}\theta p_{\text{CO}}$
Reaction R_6	$\text{Site}-\text{O} + \text{O}\,(+\,\text{Cs}) \rightleftharpoons \text{Site} + \text{CO}_2$	$N_a\tau_6 = k_{f_6}\theta_O p_O - k_{b_6}\theta p_{\text{CO}_2}$
Reaction R_7	$\text{Site} + \text{N} \rightleftharpoons \text{Site}-\text{N}$	$N_a\tau_7 = k_{f_7}\theta p_{\text{N}} - k_{b_7}\theta_N$
Reaction R_8	$\text{Site}-\text{N} + \text{N} \rightleftharpoons \text{Site} + \text{N}_2$	$N_a\tau_8 = k_{f_8}\theta_N p_{\text{N}} - k_{b_8}\theta p_{\text{N}_2}$
Reaction R_9	$\text{Site} + \text{N}\,(+\,\text{Cs}) \rightleftharpoons \text{Site} + \text{CN}$	$N_a\tau_9 = k_{f_9}\theta - k_{b_9}\theta p_{\text{CN}}$
Reaction R_{10}	$\text{Site}\,(+\,\text{Cs}) \rightleftharpoons \text{Site} + \text{C}$	$N_a\tau_{10} = k_{f_{10}}\theta - k_{b_{10}}p_{\text{C}}$
Reaction R_{11}	$2\,\text{Site}\,(+\,2\,\text{Cs}) \rightleftharpoons 2\,\text{Site} + \text{C}_2$	$N_a\tau_{11} = k_{f_{11}}\theta^2 - k_{b_{11}}\theta^2 p_{\text{C}_2}$
Reaction R_{12}	$3\,\text{Site}\,(+\,3\,\text{Cs}) \rightleftharpoons \text{Site} + \text{C}_3$	$N_a\tau_{12} = k_{f_{12}}\theta^3 - k_{b_{12}}\theta^3 p_{\text{C}_3}$

One more equality, necessary to solve equations, comes from the fact that $\theta = $ (Number of free sites)$/N_S$, $\theta_O = $ (Number of sites occupied by O)$/N_S$, $\theta_N = $ (Number of sites occupied by N)$/N_S$ and (Number of free sites) + (Number of sites occupied by O) + (Number of sites occupied by N) $= N_S$ leads to:

$$\theta + \theta_O + \theta_N = 1 \tag{1}$$

The reaction constants are defined by Duffa as functions of the temperature according to Arrhenius law whose parameter values are defined in literature [1]. It's important to note that, contrary to Zhluktov model, partial pressures are scaled by P_0. The values of reaction 1 and 9 constants were modified according to the literature [7, 8, 9].

On the one hand, for direct reactions constants k_{f1} and k_{f9}, the corrections of the pre-exponential values are due to verification of the numerical values from source's literature [8, 7] of Duffa and consist in :

- $k_{f1} = k_{f1-Duffa} \times N_a$
- $k_{f9} = k_{f9-Duffa}/P_0$ since the model is expressed in dimensionless pressure.

On the other hand, the corrections made to the k_{b9} coefficients are extracted from a curve fit in the form $A \times T^n \times exp(-E_a/T)$ based on corrected equilibrium constants computations. To this purpose, the NIST-JANAF [9] tables provide the formation constants (K_f) of Cs, CN and N species as a function of temperature. The equilibrium constant K of reaction 9 can be calculated from equation 2. Knowing, k_{f9} and K as a function of temperature, the coefficient k_{b9} can be calculated by the relation $k_{b9} = k_{f9}/K_9$. The coefficients values retained for the curve fit are : $A = 5.6753 \times 10^{25}$, $n = -1.1055$ and $Ea = 1825.5$.

$$K = \exp(ln(K_{f_{\text{CN}}}) - ln(K_{f_{\text{N}}}) - ln(K_{f_{\text{Cs}}})) \tag{2}$$

2.2 Zhluktov Model

Zhluktov model [2] differs from Duffa's one by taking into account more detailed oxidation reactions at the expense of nitridation reactions. However, it is assumed that nitridation reactions have a smaller effect on the regression speed of the wall. Reactions are described in the Table 2. Moreover, Zhluktov express the inverse kinetic constants directly as a function of the dissociation constants [8] of the gas species.

Table 2: Surface reactions of Zhluktov model [2]

	Reactions' expression	Reactions' rate
Reaction R_1	$O + Site \Longleftrightarrow Site-O$	$N_a \cdot \tau_1 = k_{f_1} \cdot \left(p_O \cdot \theta - \frac{\theta_O}{K_1} \right)$
Reaction R_2	$O_2 + 2\,Site \Longleftrightarrow 2\,Site-O$	$N_a \cdot \tau_2 = k_{b_2} \cdot \left(K_2 \cdot p_{O_2} \cdot \theta^2 - \theta_O^2 \right)$
Reaction R_3	$O_2 + Site \Longleftrightarrow Site-O + O$	$N_a \cdot \tau_3 = k_{f_3} \cdot \left(p_{O_2} \cdot \theta - \frac{p_O \cdot \theta_O}{K_3} \right)$
Reaction R_4	$CO_2 + Site \Longleftrightarrow Site + CO$	$N_a \cdot \tau_4 = k_{f_4} \cdot \left(p_{CO_2} \cdot \theta - \frac{p_{CO} \cdot \theta_O}{K_4} \right)$
Reaction R_5	$Site-O\,(+Cs) \Longleftrightarrow Site + CO$	$N_a \cdot \tau_5 = k_{f_5} \cdot \left(\theta_O - \frac{p_{CO} \cdot \theta}{K_5} \right)$
Reaction R_6	$Site-O + O\,(+Cs) \Longleftrightarrow Site + CO_2$	$N_a \cdot \tau_6 = k_{f_6} \cdot \left(p_O \cdot \theta_O - \frac{p_{CO_2} \cdot \theta}{K_6} \right)$
Reaction R_7	$2\,Site-O\,(+Cs) \Longleftrightarrow 2\,Site + CO_2$	$N_a \cdot \tau_7 = k_{f_7} \cdot \left(\theta_O^2 - \frac{p_{CO_2} \cdot \theta^2}{K_7} \right)$
Reaction R_8	$Site\,(+Cs) \Longleftrightarrow Site + C$	$N_a \cdot \tau_8 = k_{b_8} \cdot \theta \cdot (K_8 - p_C)$
Reaction R_9	$2\,Site\,(+2\,Cs) \Longleftrightarrow 2\,Site + C_2$	$N_a \cdot \tau_9 = k_{b_9} \cdot \theta^2 \cdot (K_9 - p_{C_2})$
Reaction R_{10}	$3\,Site\,(+3\,Cs) \Longleftrightarrow 3\,Site + C_3$	$N_a \cdot \tau_{10} = k_{b_{10}} \cdot \theta^3 \cdot (K_{10} - p_{C_3})$
Reaction R_{11}	$Site + N \Longleftrightarrow Site-N$	$N_a \cdot \tau_{11} = k_{f_{11}} \cdot \left(p_N \cdot \theta - \frac{p_{\theta_N}}{K_{11}} \right)$
Reaction R_{12}	$Site-N + N \Longleftrightarrow Site + N_2$	$N_a \cdot \tau_{12} = k_{b_{12}} \cdot (K_{12} \cdot p_N \cdot \theta_N - p_{N_2} \cdot \theta)$

In this model, different activation temperature exists [8, 10, 2] for direct reactions 5, 6 and 7 and different numerical expression exists for constant reactions 1 and 11. In this paper, due to the objective of modeling carbon phenolic ablation in an atmospheric entry, chosen value are : $T_{a5} = 40\,000\,\text{K}$, $T_{a6} = 2000\,\text{K}$, $T_{a7} = 40\,000\,\text{K}$, $\frac{1}{K_1} = Ns \cdot \left(\frac{k \cdot T}{P_0} \right) \cdot \left(\frac{2\pi \cdot m_O \cdot k \cdot T}{h^2} \right)^{\frac{1}{2}} \cdot exp\left(\frac{-T_{d1}}{T} \right)$ and $\frac{1}{K_{11}} = Ns \cdot \left(\frac{k \cdot T}{P_0} \right) \cdot \left(\frac{2\pi \cdot m_N \cdot k \cdot T}{h^2} \right)^{\frac{1}{2}} \cdot exp\left(\frac{-T_{d11}}{T} \right)$

3. Non-coupled test case

This section presents the resolution methods developed in the non-coupled simple test case of the surface chemical reactions models and associated results.

3.1 Non-coupled method

The objective of the non-coupled method is to compare the chemical reactions models on simple test case. Therefore, we have chosen to apply at boundary elementary surface the chemical composition of the air at one bar as a function of the temperature and independent of the degradation of the material. This composition, which is plot on figure 1, has been obtained by an equilibrium calculation. So the only variable will be the surface temperature. Therefore, partial pressures are no longer unknowns at the boundary surface. Moreover, we assume a stationary regime which results in equation 3:

$$\frac{d}{dt}(\theta) = \frac{d}{dt}(\theta_O) = \frac{d}{dt}(\theta_N) = 0 \qquad (3)$$

Therefore, we obtain for both models a non-linear system with 15 equations (3 plus 12 equations from table 1 or 2) and 15 unknowns (τ_i for $i \in [1, 12]$, $\theta, \theta_O, \theta_N$) with the constraint that $\theta, \theta_O, \theta_N \in [0, 1]$. To compare, among other things, the regression rates of the models, we have considered a fictive material of density $1180\,\text{kg.m}^{-3}$ and applied the approximate formula:

$$V_{\text{wall regression}} = -\frac{\dot{m_{carbon}}}{\rho_{wall}} \qquad (4)$$

with:

- $V_{\text{wall regression}}$: Regression speed of the wall m.s^{-1}

- $\dot{m_{carbon}}$: Mass flow rate of carbon kg.s^{-1}.m^{-2}

- ρ_{wall}: Volumic mass of material

ABLATIVE TPS INTERACTING WITH A HYPERSONIC FLOW
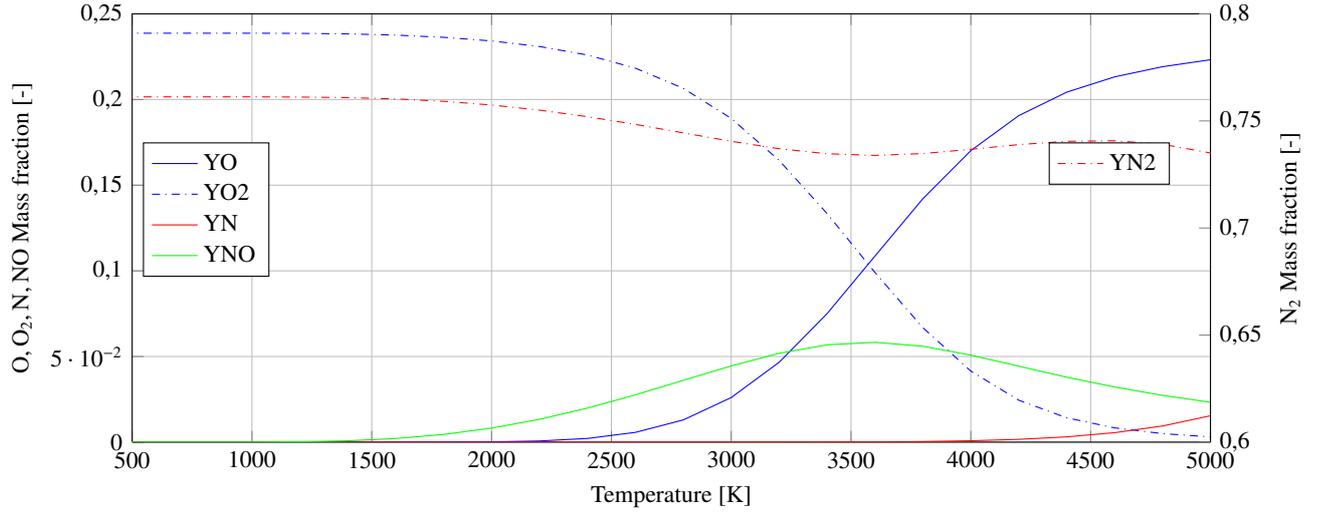
Figure 1: Major species of air composition as a function of temperature at thermochemical equilibrium at 1 bar

3.1.1 Resolution of Duffa model

The combination of the stationary regime (equation 3) and the expression of surface creation terms (tableau 1) gives :

$$
\begin{cases}
2 * \tau_1 - \tau_2 - \tau_3 - \tau_5 - \tau_6 = 0 \\
\tau_7 - \tau_8 = 0
\end{cases}
\tag{5}
$$

By choosing θ as a pivot variable, the equation 5 gives :

$$
\begin{cases}
\theta^2 \cdot \left[2 * k_{f1} * P_{O_2} - 2 * k_{b1} * tmp^2 \right] \\
+\theta \cdot \left[k_{b2} P_O + k_{b3} P_{O_2} + P_{CO_2} (k_{b4} + k_{b6}) + k_{b5} P_{CO} \right] \\
+\theta \cdot tmp \left[4 * k_{b1} + k_{f2} + k_{f3} P_O + k_{f4} P_{CO} + k_{f5} + k_{f6} P_O \right] \\
+1 \cdot \left[-2 * k_{b1} - k_{f2} - P_O \left(k_{f3} + k_{f6} \right) - k_{f4} P_{CO} - k_{f5} \right] \\
\quad = 0
\end{cases}
\tag{6}
$$

with:

$$
tmp = 1 + \frac{k_{f7} P_N + k_{b8} P_{N_2}}{k_{b7} + k_{f8} P_N}
$$

$$
\theta_N = \theta \cdot (tmp - 1)
$$

$$
1 = \theta + \theta_N + \theta_O
$$

This second order system can be solved under the condition that the partial pressures of each species are known. About the non-coupled method these values are given by the calculation of the composition of the air at 1 bar and equilibrium. About the coupled method, which is describe later, these partial pressures are determined using the fluid mechanics code.

3.1.2 Resolution of Zhluktov model

Similarly to Duffa's model, Zhluktov's model is solved by chosing θ as a pivot variable and assuming a stationary regime. Likewise the Duffa model, this second order system can be solved under the condition that the partial pressures of each species are known.

3.2 Non-coupled method results

(a) Regression speed due to surface reactions

(b) Free fraction sites
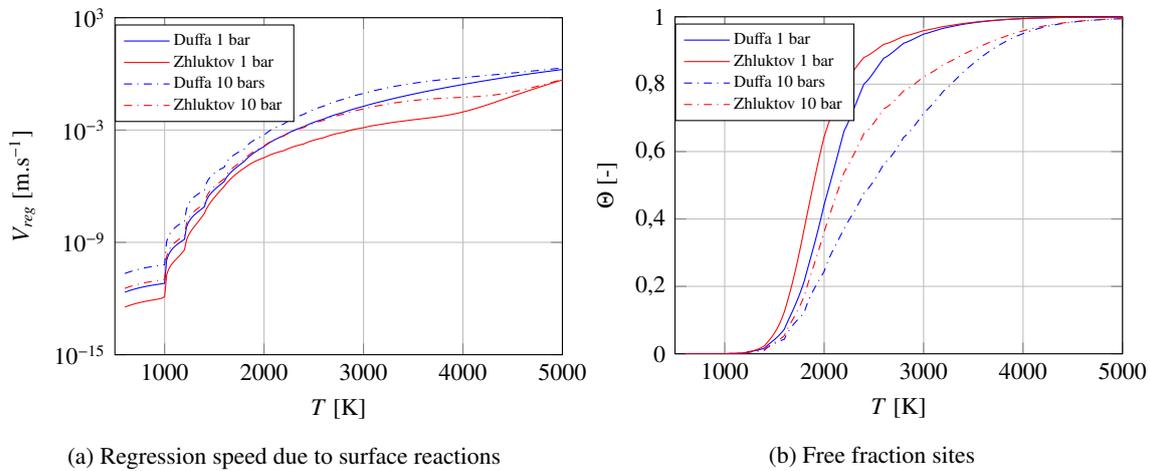
Figure 2: Non-coupled results

Figure 2 represents regression speed and fraction of free sites evolution for Duffa and Zluktov models. Globally, the behavior of the two models are similar. The curves obtained are consistent with the expectations of the literature. Indeed, at low temperature the sites are experimentally all occupied by oxygen and are released with the increase of the temperature since the kinetics of the reactions becomes extremely fast by making react immediately the oxygen atoms available. Moreover, on figure 2a, the activation of the different reactions can be observed by the changes of slope. At low temperature, the regression rate is close to zero. Then, for a temperature close to 1000 K, the chemical reactions are activated and increase the regression speed of the surface. For temperatures above 1800 K, the regression rate keep increasing exponentially with temperature. A plateau is expected due to the fact that from these temperatures, the kinetics of oxidation are controlled by diffusion of chemical species through the boundary layer. However, in this simple case, the results do not reproduce this diffusion effect since the composition of the fluid at the wall is imposed (no CO or CO_2). For temperature above 2500 K, the phenomenon of sublimation becomes preponderant and exponentially increasing.

4. Coupled method

The second method used to compare both models is to take into account the interaction between the flow and the reacting surface. To do it, the CFD platform Two phase reagents flow calculation for energetic (CEDRE) using CHARME solver is coupled with the composite material degradation solver MoDeTheC in which chemicals reactions models have been implemented. The resolution method previously presented are extended in MoDeTheC to be done on every elementary boundary surface where surface ablation is activated. To ensure realistic calculation, simulation are applied on RAMC-I experiment.

4.1 Test case presentation

The RAMC-I flight carried out by NASA in the 60s aimed to study the phenomena at the origin of the "*black out*" which, because of the ionization of the flow around a reentry body, blocks the radio communications between it and the ground station. The sphere-cone-shaped probe, as shown in figure 3, has its nose made of an ablatable composite material: NARMCO 4028 (phenolic carbon)[5].
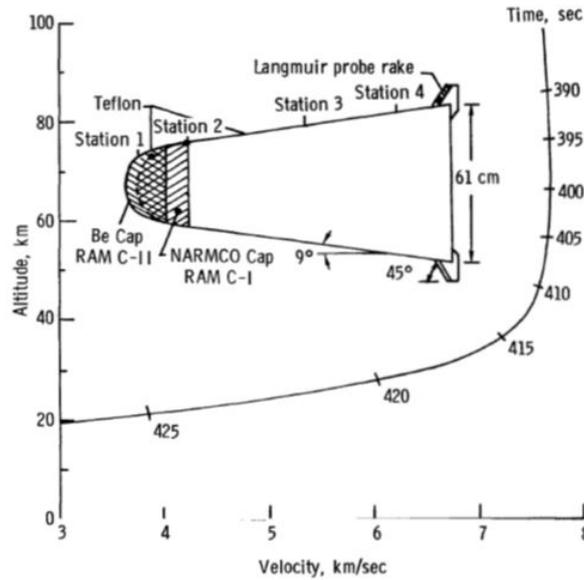
Figure 3: Shape and wall materials of RAM-C I and II probes as well as the speed / altitude curve [5]

Figure 3 also describes the trajectory. However, in this study, only one point of the trajectory of the probe RAMC-I is studied. It is the point located at an altitude of 40 km, whose characteristics are detailed in Table 3

Table 3: Flight conditions of the RAMC-I probe at an altitude of 40 km

Flight time [s]	Altitude [km]	Speed [m.s^{-1}]	Pressure [Pa]	Temperature [K]	Density [kg.m^{-3}]	Mach
412.6	40	7391	273.2	246.14	$3.966E-3$	23.474

4.2 NARMCO 4028 material

The material of the ablating part of the probe is a composite material of type NARMCO 4028 in the so-called "virgin" state (Mv). During its heating, this one degrades by the whole of ablation phenomena. The phenomena taken into account in the current simulation are the pyrolysis and the surface reactions of oxidation, nitridation and sublimation previously described. With the increase of temperature, the virgin material will first pyrolyze giving char which is then oxidize, nitrate and sublimate. The properties of the virgin and char materials configured in the MoDeTheC code are summarized in the table 4:

Table 4: Properties of NARMCO 4028 material

	Virgin material	Char Material
Volumic masse kg.m^{-3}	1312	993
Specific heat J.kg^{-1}	1500	2000
Conductivity W.m^{-1}.K	1	10
Emissivity	0.7	
Permeability	Kozeny-Carman Model $K_{p0} = 5.2 \times 10^{-12}\,\text{m}^2$ $K_{pm} = 6.5 \times 10^{-14}\,\text{m}^2$	

The kinetics of the pyrolysis reaction extracted from the literature [1] is described as follows:

$$\text{Virgin material} \xrightarrow{^{\circ}\text{K}} 0.5\,\text{char} + 0.25695\,CO + 0.18247\,CO_2 + 0.03235\,H_2O + 0.02823\,H_2$$
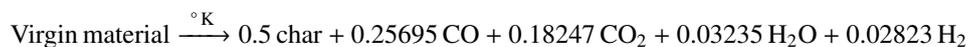
Reaction rate of pyrolysis follow Arrhenius' laws ($A \times T^n \times exp(-E_a/(R*T))$) of which the parameters are:

- Pre-exponential constant $A = 1390\,\text{s}^{-1}$

8

- Activation energy $E_a = 67\,098.015\,\text{J.mol}^{-1}$

- Order of the reaction $n = 1.29$

- Standard enthalpy of reaction $= 465\,000\,\text{J/mol}$

4.3 Earth atmosphere model

The simulation of the re-entry of the probe RAMC-I is carried out in Earth's atmosphere by taking as values of temperatures, pressures and densities those provided by the atmospheric model COSPAR-CIRA [11]. The initial upstream mass fractions of oxygen and nitrogen are respectively 0.23 and 0.77. The model of atmosphere retained is composed of 11 species from Park [7] to which are added the 8 species coming from the decomposition of the material:

$$\left[\underbrace{N, N^+, N_2, N_2^+, NO, NO^+, O, O^+, O_2, O_2^+, e}_{\text{Atmosphere omposition}}, \underbrace{CO, CO_2, H_2, C_2, C_3, H_2O, CN, C}_{\text{Degradation products}} \right]$$
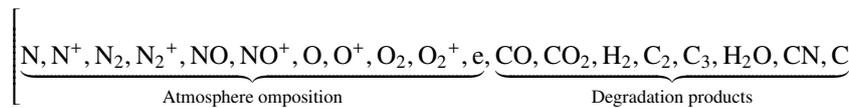
Considering the atmosphere as a perfect gas mixture, 25 reactions are taken into account according to the Park's model [7] and it's assumed that ablation products are inert with the atmosphere species.

4.4 Geometry and mesh

Two distinct calculation domains is considered. the domain representing the flow around the reentry body which is processed by CHARME and the domain representing the material part of the reentry body which is processed by MoDeTheC.

The angle of attack is assumed to be zero along the trajectory and the geometry of the probe is axisymmetric. The two domains presented in the figure 4 were meshed in 2D-axisymmetric.
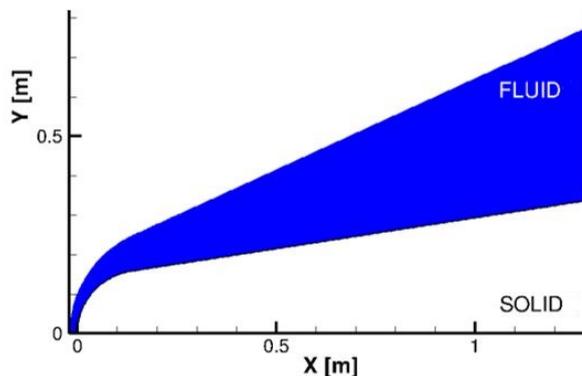
Figure 4: Axisymmetric calculation domains

Fluid domain : Figure 5 illustrates the geometry of the fluid computation domain and its mesh. It is a structured one and consists of 25425 quadrangles. Particular attention has been paid to the alignment and refinement of the mesh according to the shock at the stagnation line. In addition, the mesh was also refined at the wall of the probe (boundaries "NOSE" and "BODY") with a size of the first mesh of 2 microns in order to best represent the boundary layer. These points are crucial to correctly simulate the heat fluxes at the wall with the CHARME solver.

ABLATIVE TPS INTERACTING WITH A HYPERSONIC FLOW
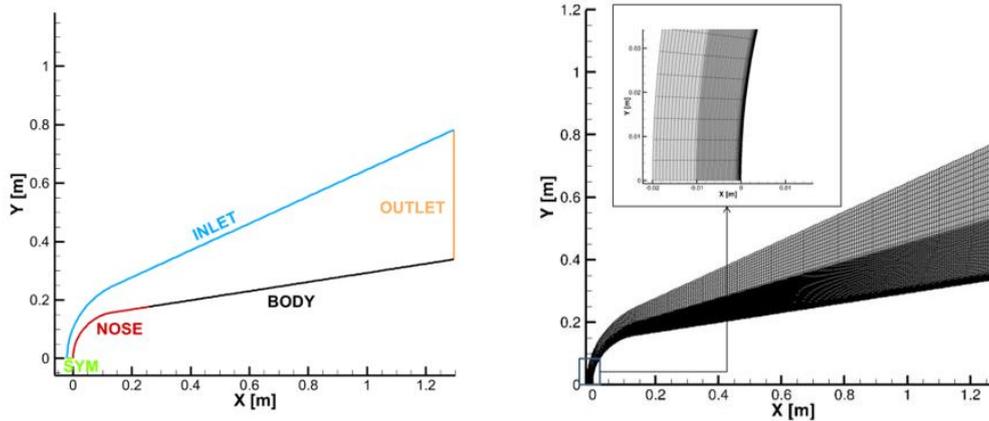
Figure 5: Geometry and mesh of the "fluid" computational domain

Solid domain :   Figure 6 shows the geometry and the mesh for the solid domain. The mesh is hybrid with a layer of quadrangles at the boundaries NOSE and BODY and triangles for the rest of the field. The mesh is composed of 3094 elements. The surface chemical degradation phenomena is only modeled on the NOSE part and pyrolysis is modeled on the whole solid domain. It will be noted that the meshes are in conformity at the boundary conditions NOSE and BODY between the two domains of computation.
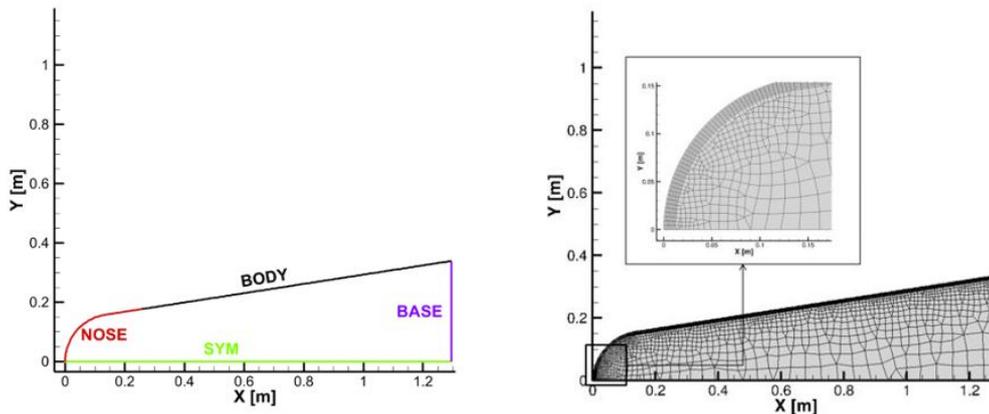
Figure 6: Geometry and mesh of the "solid" computational domain

4.5 Spatial discretization and temporal integration

CHARME solver :   The spatial discretization is done at order 2 with a finite volume approach. The Euler flow scheme used is the AUSM+ scheme with an additional dissipation based on the velocity jump through the shock. The time integration is performed with a first-order implicit time scheme solved with the GMRES method and with a local time step based on CFL=1.

MoDeTheC solver :   In the MoDeTheC solver, a first-order operator splitting scheme is used:

- heat diffusion fluxes and chemical source terms are first integrated with an implicit Euler scheme (order 1) ;

- the advection fluxes of the pyrolysis gas are then integrated with an implicit Euler scheme (order 1), subdivided by limiting the time step by a unit CFL number.

The computation of the variables and their gradients at the faces for the diffusive flows is based on the second order scheme of Leterrier [12], also implemented in the CHARME solver. The calculation of the variables at the faces for the advective flows is based on a second order TVD scheme with the Van Leer limiter.

10

4.6 Boundaries conditions

Fluid domain: With the notations of the figure 5, the modeling of boundary conditions INLET is a supersonic inlet with the conditions given in the table 3, OUTLET is a supersonic outlet, SYM is a symmetry with sliding condition and NOSE is the wall with degradation. The boundary conditions of this wall, in particular the blown flow rate and the wall temperature, come from the coupling with the MoDeTheC solver.

Solid domain: With the notations of the figure 6, the modeling of boundary BODY is a wall with exchange of temperature, heat and gas flow (advection) and pressure without degradation, BASE is an adiabatic wall, SYM is a symmetry and NOSE is the wall with degradation.

4.7 Coupling CHARME - MoDeTheC

To simulate a flight point of the re-entry trajectory of the probe, it is necessary to carry out several stages of calculation in order to reproduce the history of what the probe experienced before the considered flight point. This facilitates the coupling between the two codes by progressively decreasing the gap existing between the quantities of the two domains.

The methods of calculation and coupling are therefore:

1. A first CHARME calculation to obtain a stationary solution of the flow around the probe at the considered altitude by assuming the boundaries conditions NOSE and BODY as an isothermal wall at 500 K. This solution is obtained with a time step of 1×10^{-5} s.

2. A second calculation is performed by activating the coupling between CHARME and MoDeTheC without activating the surface material degradation on the NOSE and BODY limits and pyrolysis volumic degradation. CHARME sends the pressure, the composition of the flow at wall surface and the convective heat flux to MoDeTheC. Time step for CHARME, MoDeTheC and coupling are equals to 1×10^{-5} s. Simulation time = 1 s

3. A third calculation is performed with the same coupling plus the pyrolysis reaction of the material. In this step, and on the limits NOSE and BODY, CHARME sends the pressure at the wall as well as the composition and the convective heat flux to MoDeTheC. MoDeTheC sends the temperature of the wall as well as the temperature, the composition and the mass flow of the blown gases to CHARME. Time step for CHARME, MoDeTheC and coupling are equals to 1×10^{-5} s. Simulation time = 3.2 s

4. Finally, the last calculation is performed with the coupling activated as well as all degradation sources activated: Pyrolysis for the entire probe and oxidation, nitridation and sublimation surface reaction for the NOSE boundary. From now on, pressure, composition of the flow at wall surface and convective heat flux are sent to MoDeTheC on NOSE and BODY boundary. Compared to the previous step, MoDeTheC sends on NOSE boundary the mass and energy flux due to degradation to the CHARME solver. The gases ejected from the wall are assumed to be at wall temperature. The solver takes into account all the energy fluxes at the fluid/solid interface (convective flux coming from the CHARME solver, conductive flux at the wall, radiative flux emitted by the wall as well as the energy fluxes linked to the mass fluxes) to determine the heating of the material. From a temporal point of view, the integration sequence starts with CHARME which performs 1 iteration with a time step of 1×10^{-6} s. At the same time, MoDeTheC performs 1 iteration with a time step of 1×10^{-6} s (note the temporal consistency between CHARME and MoDeTheC). At the end of the time integration of each code, the codes exchange the quantities on the boundary conditions NOSE and BODY. The three previous actions are carried out in order to ensure a simulation on a physical duration of 0.03 s. The mesh deformation of fluid domain is not taken into account contrary to solid domain where mesh displacement is activated. Therefore, the physical time of simulation has been limited. Indeed, the objective is that the wall regression should not be too large (a few mm) for the assumption of a fixed mesh size of the flow to be acceptable.

4.8 Results

The results obtained in the simulation of the probe RAMC-I are presented in the subsections below. In particular, results in the stagnation area are discussed.

ABLATIVE TPS INTERACTING WITH A HYPERSONIC FLOW

(a) Temperature and mesh after 0.05 s of simulation

(b) Gaz displacement streamlines and temperature
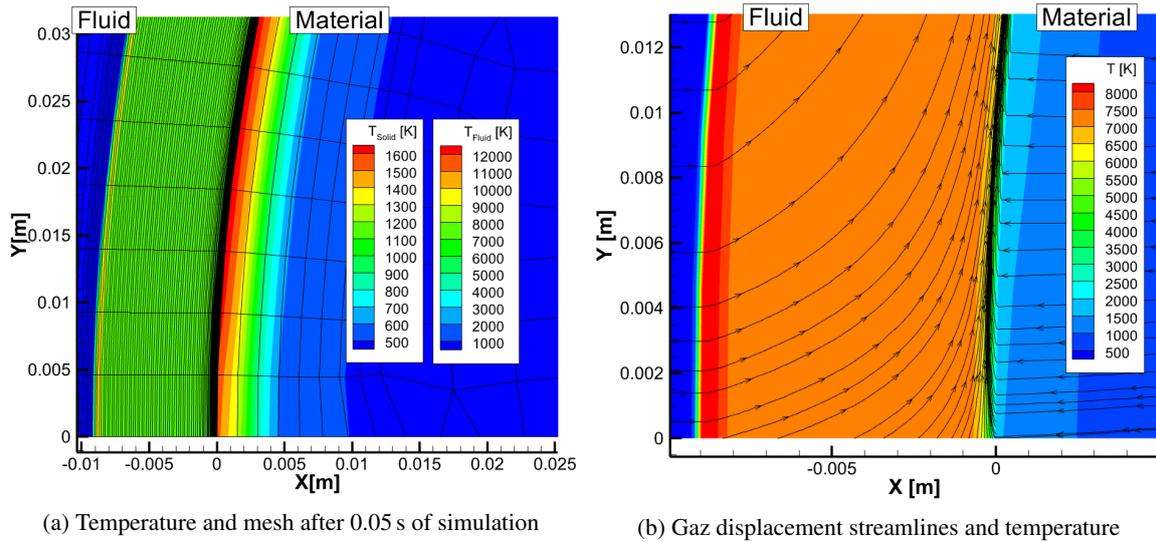
Figure 7: Volumic results of RAMC-I simulation with Duffa chemical surface reaction

Figure 7a shows the temperature in the fluid and solid and the mesh displacement. It allows to validate our hypothesis of very small mesh displacement on the MoDeTheC side for the coupling with CHARME. The shock layer temperature is in the range from 6000 K to 7000 K and the material reaches about 1700 K. At these temperature levels, pyrolysis is activated in volume, and mainly oxidation on the surface. We can observe the flow lines linked to the outgassing of the wall. By pushing back the external flow, this outgassing causes a very slight displacement of the shock. It would be interesting to treat a flight point at lower altitude to see if we reach sufficient temperatures to sublimate.

(a) Temperature and pyrolysis reaction advancement after pyrolysis step

(b) Porosity and pyrolysis reaction advancement after pyrolysis step
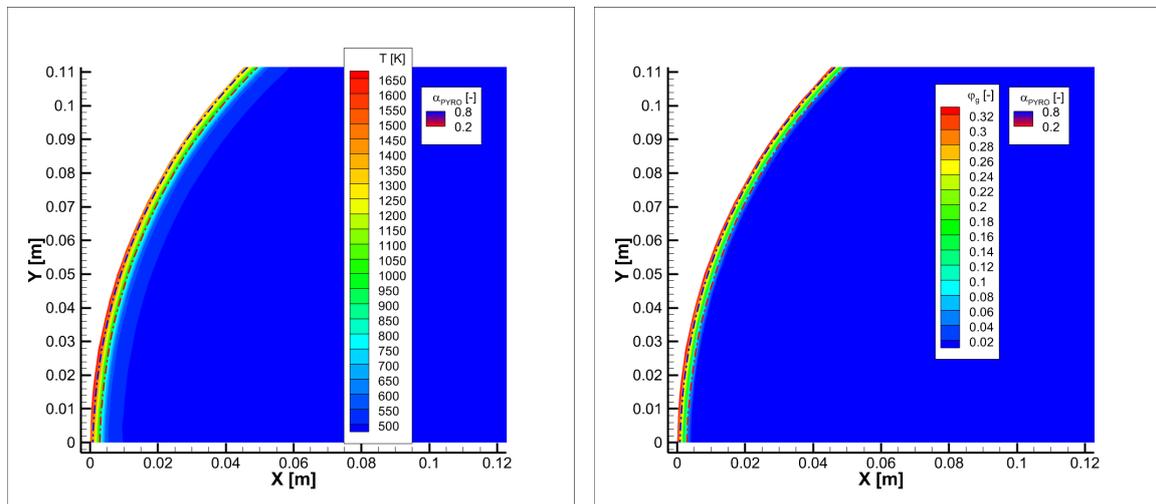
Figure 8: Temperature, porosity and pyrolysis reaction advancement after pyrolysis step without ablation

Figure 8 confirms again the validity of our results since we can observe the advance of the pyrolysis fronts which are followed by a material whose porosity converges to 0.33. This value is in line with our expectations since generally the porosity of degraded carbon composites is around 0.3.

(a) NOSE surface temperature profil and heat flux

(b) Pyrolysis and ablation mass flux
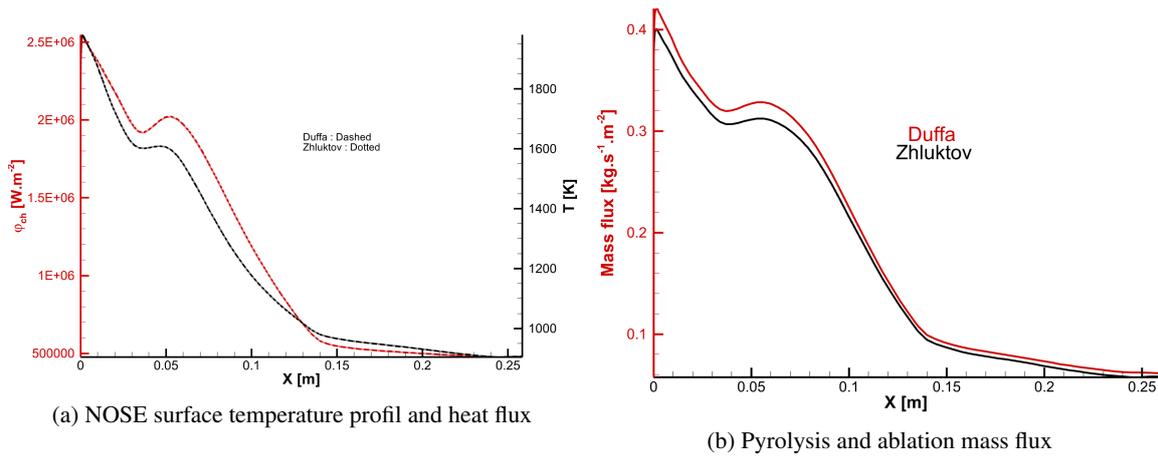
Figure 9: Surfacic results of RAMC-I simulation

Figure 9 plots the profile of temperature, heat fluxes, and mass flux due to pyrolysis and ablation on the NOSE boundary surface. The hump observed for x=0.55 m or an angle of 50° corresponds to the transition of the flow to a turbulent regime transmitting a higher heat flux than if the flow was considered as totally laminar. The models of Duffa and Zhluktov are very similar on temperature, mass flux and heat flux profile.
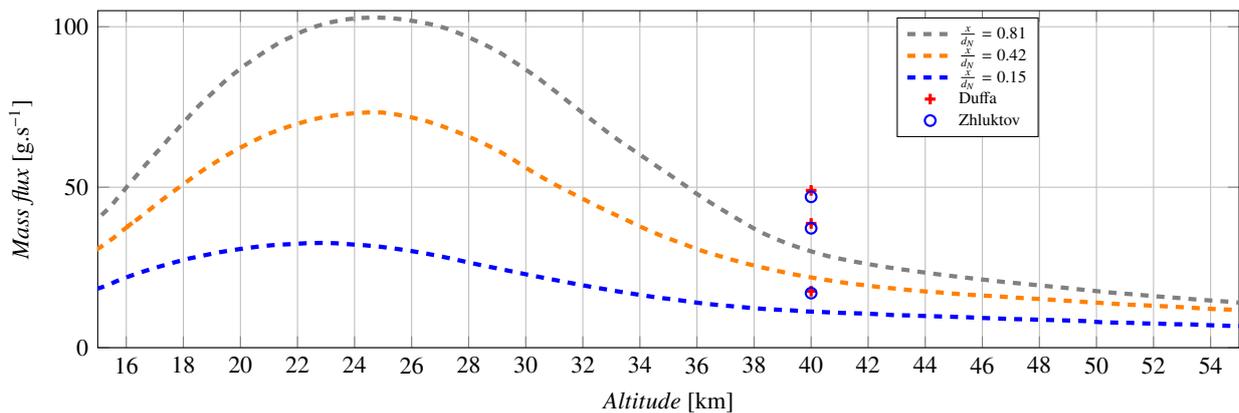
Figure 10: Calculated mass flux at 40 km versus literature data [5]

Figure 10 compares the mass flux due to pyrolysis and ablation calculated at the altitude of 40 km with literature's data [5]. Literature's data calculate the mass flux over NOSE at different altitude and over different integrated surface aera of the nose cap to the several body stations. Ablation flow rate has been calculated over three different body stations at x/d_N equals to 0.81, 0.42 and 0.15 where d_N is the diameter of the spherical portion of the probe (For RAMC-I: $d_N = 31.90$ cm [13]). Hence, the simulation gives a total mass flux that is representative for that given altitude. It is important to note that contrary to the literature, turbulence is taken into account in the calculations and it could explain the fact that the results are slightly higher. Moreover, considering the temperatures on the surface and in the material, the pyrolysis phenomenon is here preponderant, especially in the mass flux. The slightly higher values of the Duffa model are consistent with the uncoupled test case which showed a higher regression speed for a given temperature of this model.

5. Conclusion

The interaction between a flow and an ablatable wall during an atmospheric reentry is complex to model because of the diversity of the physical phenomena involved. Among these multi-physical phenomena, one of the objectives of this paper was to improve the consideration of oxidation, nitridation and sublimation reactions by implementing reaction models. Two models have been added in the MoDeTheC solver. The coupling between the fluid mechanics code CHARME solver and MoDeTheC allowed to model and simulate the interaction between the flow and an ablatable wall during the atmospheric reentry of a probe. The first results obtained, in terms of pyrolysis and ablation mass flux,

are conclusive and consistent with the literature. On the other hand, the models are still investigated to provide the gas production terms. The difficulty here lies in obtaining all the data on the test conditions and materials, which the literature alone does not generally allow. Indeed, the number of experimental installations for ablation is very limited and they are very expensive to implement. In future works, other flight points of RAMC-I will be studied and other test cases such as those on the carbon-phenolic material of the missions Pacemaker [6] or even flight tests carried out by the NASA [14], will be studied to test the robustness of the models.

References

[1] G. Duffa, *Ablative Thermal Protection Systems Modeling*, American Institute of Aeronautics and Astronautics, Inc., Washington, DC, illustrate édition (@may 2013), `https://arc.aiaa.org/doi/book/10.2514/4.101717`.

[2] S. V. Zhluktov & T. Abe, *Viscous Shock-Layer Simulation of Airflow past Ablating Blunt Body with Carbon Surface*, Journal of Thermophysics and Heat Transfer, 13 (1), pp. 50–59 (@jan 1999), `https://arc.aiaa.org/doi/10.2514/2.6400`.

[3] V. Biasi, *Modélisation thermique de la dégradation d'un matériau composite soumis au feu*, Thèse de doctorat, Institut Supérieur de l'Aéronautique et de l'Espace (ISAE) (2014), `https://hal.archives-ouvertes.fr/tel-01234928`.

[4] T. Soubrie, *CEDRE : Calcul d'Écoulements Diphasiques Réactifs pour l'Énergétique* (2022), `https://cedre.onera.fr/`.

[5] P. W. Huber, J. C. J. Schexnayder & J. S. Evans, *Calculation of electron concentration for a blunt body at orbital speeds and comparison with experimental data*, Rapport Technique NASA Langley Research Center n^o L-6705, Hampton, VA (1971), `http://hdl.handle.net/2060/19710016599`.

[6] T. E. Walton & W. G. Witte, *Flight test of carbon-phenolic on a spacecraft launched by the pacemaker vehicle system*, Rapport Technique NASA Langley Research Center n^o L-8098, Hampton, VA (1972), `https://ntrs.nasa.gov/citations/19720011982`.

[7] C. Park, *Review of chemical-kinetic problems of future NASA missions. I - Earth entries*, Journal of Thermophysics and Heat Transfer, 7 (3), pp. 385–398 (@jul 1993), `https://arc.aiaa.org/doi/10.2514/3.431`.

[8] Y.-K. Chen & F. Milos, *Finite-Rate Ablation Boundary Conditions for a Carbon-Phenolic Heat-Shield*, Dans *37th AIAA Thermophysics Conference*, pp. 1–16, Reston, Virigina, American Institute of Aeronautics and Astronautics (@jun 2004), `https://arc.aiaa.org/doi/10.2514/6.2004-2270`.

[9] T. C. Allison, *NIST-JANAF Thermochemical Tables*, National Institute of Standards and Technology (2013), `https://janaf.nist.gov/`.

[10] Y.-K. Chen & F. S. Milos, *Navier-Stokes Solutions with Finite Rate Ablation for Planetary Mission Earth Reentries*, Journal of Spacecraft and Rockets, 42 (6), pp. 961–970 (@nov 2005), `https://arc.aiaa.org/doi/10.2514/1.12248`.

[11] E. L. Fleming, S. Chandra, J. Barnett & M. Corney, *Zonal mean temperature, pressure, zonal wind and geopotential height as functions of latitude*, Advances in Space Research, 10 (12), pp. 11–59 (@jan 1990), `https://linkinghub.elsevier.com/retrieve/pii/027311779090386E`.

[12] N. Leterrier, *Discrétisation spatiale en maillage non-structuré de type général*, Thèse de doctorat, Université Pierre et Marie Curie (Paris VI) (2003), `http://www.theses.fr/2003PA066192`.

[13] P. W. Huber, N. D. Akey, W. F. Croswell & C. T. Swift, *The Entry Plasma Sheath and Its Effects on Space Vehicle Electromagnetic Systems*, Rapport Technique Langley Research Center, Hampton, Virginia (1970), `https://ntrs.nasa.gov/citations/19710011626`.

[14] R. N. Hopko, B. Rashis, C. W. Winters & W. G. Witte, *A free-flight investigation of ablation of a blunt body to a mach number of 13.1*, Rapport Technique NASA Langley Research Center Hampton, VA, United States n^o December, Hampton, Va (1962), `https://ntrs.nasa.gov/citations/19630000924`.